Results divided into logical sections

Results

Device structure. We have recently reported on perovskite-based thin-film photovoltaic devices with an architecture evolved from the solid-state dye-sensitized solar cells, where holes are collected through the metal cathode and electrons through the FTO anode[10]. In this configuration, a thin film of mesoporous alumina is deposited over compact TiO_2-covered FTO substrates to aid the perovskite film formation[10], then an organic hole transporter is deposited over the formed structure to provide a hole selective contact. Henceforth, this configuration will be referred to as 'regular' and the cell architecture, which represents the focus of the work here shall be termed 'inverted'. Typical materials used in organic photovoltaics as hole selective contacts are PEDOT:PSS, V_2O_5 and NiO[17,18], while usually PCBM and more recently poly[(9,9-bis(3′-(*N*,*N*-dimethylamino)propyl)-2,7-fluorene)-alt-2,7-(9,9–dioctylfluorene)] (PFN)[19] are used as electron acceptors or electron selective contacts. In order to determine whether these materials are compatible to act as electron and hole acceptors within the perovskite-based devices, we first estimate photoluminescence (PL) quenching of the perovskite emission in thin-film bi-layers, as has become routine in all organic solar cells[20]. We present this data in Fig. 1 and the results are summarized in Table 1. All the *p*-type layers chosen in this work

Rationale / Findings / Transition

1–2 figures per Results section

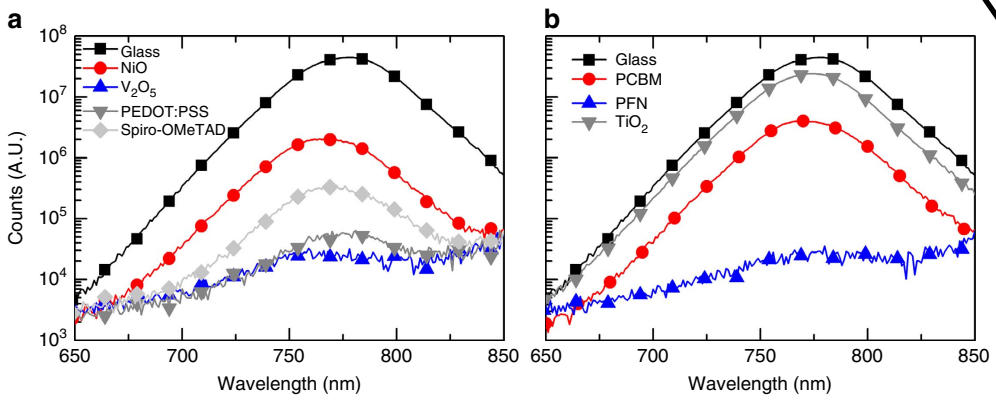

Figure 1 | Photoluminescence response for $CH_3NH_3PbI_{3-x}Cl_x$ perovskite films coated with *p*- and *n*-type layers to ascertain their charge transfer compatibility. (**a**) Steady-state photoluminescence spectra of *p*-type quenchers and (**b**) *n*-type quenchers of perovskite films processed in a bi-layer configuration. For the *p*-type quenchers, the perovskite was coated on top of the *p*-type collection layers, whereas for the *n*-type quenchers, the perovskite was first processed on glass slides, then the *n*-type charge collection layers were spin coated on top. Perovskite excitation at 530 nm was performed from the opposite side of the quencher.

quench the perovskite steady-state PL more efficiently than the archetypal 2,2′,7,7′-Tetrakis[*N*,*N*-di(4-methoxyphenyl)amino]-9,9′-spirobifluorene (spiro-OMeTAD) *p*-type hole conductor previously employed in the MSSCs, with similar values for PEDOT:PSS and V_2O_5 of 99.8% quenching efficiency. All the *n*-type layers exhibit significantly higher quenching rates than the TiO_2 compact layers previously employed. Our observation of enhanced PL quenching with PCBM, is consistent with our previous work where we looked at electron transfer from the perovskite absorber to fullerene self-assembled monolayers, indicating that organic electron and hole acceptors are highly effective when interfaced with the perovskite absorbers[21]. All the cells fabricated in this work utilize a spin coated PCBM layer as the *n*-type contact, since solar cells fabricated with a PFN interlayer yielded an extremely poor photovoltaic performance.

When applied to devices, NiO and V_2O_5 *p*-type layers resulted in rather poor photovoltaic performance (Supplementary Fig. S1), showing signs of high series resistance and for V_2O_5 a low shunt resistance in the *J*–*V* curves. This is likely to arise in part from extremely poor perovskite film formation upon the substrate, with very poor surface coverage (Supplementary Fig. S2). This will enable direct contact of the PCBM *n*-type layer with the *p*-type metal oxide, presenting a shunting path. In addition, the high series resistance may arise from low conductivity of the *p*-type oxide, suggesting improvements could be made by controlling the conductivity or doping density in the *p*-type oxide, and improving the film formation of the perovskite upon the flat metal oxide layers. In contrast, when a thin PEDOT:PSS layer is used as the *p*-type contact, a solid perovskite absorber layer exhibiting over 95% surface coverage is achieved, as estimated from scanning electron microscopy (SEM) images, and the conductivity of the PEDOT:PSS is controlled and high. This results in good photovoltaic properties when a bi-layer of PCBM and compact TiO_x is employed as the *n*-type charge collection layer. The origin of the different perovskite film formation characteristics on the different *p*-type layers is not completely understood at this moment and will be the subject of a future study, but is likely to originate from differences in surface roughness and perovskite/surface interaction energy[22]. To be able to process these structures in air, the top interlayer of TiO_x was necessary to achieve a stable electronic contact with the top Al anode (Supplementary Fig. S3)[23]. A cross-sectional SEM image of an optimized device is presented in Fig. 2.

Table 1 | Steady-state photoluminescence quenching efficiency.

p-type layers		n-type layers	
NiO	95	PCBM	91
V_2O_5	99.8	PFN	99.8
PEDOT:PSS	99.8	TiO_2	47
Spiro-OMeTAD	99.1		

The photoluminescence quenching from the perovskite was quantified for both *p*- and *n*-type charge collection layers contacting the perovskite absorber. The quenching efficiency was calculated by integrating the photoluminescence spectra over wavelength and comparing with the neat perovskite layer. We note that this is not measured in an integrating sphere, so only represents an estimation of the quenching efficiency.

Photovoltaic performance. We show the photovoltaic performance of the inverted device structure in comparison with that of the regular MSSC device architecture (composed of a compact TiO_2 electron accepting layer, low temperature processed mesoporous alumina film filled with perovskite absorber and spiro-OMeTAD as the hole transporting layer) in Fig. 3. The best performing device with the inverted architecture achieved a short-circuit photo current approaching 16 mA cm^{-2}, open-circuit voltages of over 0.9 V and 9.8% PCE, closely matching initial reports with devices based on the standard architecture. We also stress that this is achieved in a planar configuration, where no nanostructured scaffold is present and the total active layer thickness is around 300 nm. This good operation of the solid perovskite layer is consistent with our recent results where a planar heterojunction of a similar thickness composed of TiO_2/$CH_3NH_3PbI_{3-x}Cl_x$/Spiro-OMeTAD delivered over 15% PCE[14]. The PCE value shown here for inverted perovskite solar cells is higher than the best published single junction organic solar cells[19,24], similar to the highest efficiencies for a-Si, and compares favourably with early reports of alternative thin-film technologies such as copper indium gallium (di) selenide, cadmium telluride[25], with significant further improvements expected in the very near future[15]. A histogram for the PCE of a set of around 40 devices is also shown in Supplementary Fig. S4 as well as the photovoltaic performance of an inverted device under a series of light intensities from full AM 1.5 sunlight conditions to low <1% sunlight irradiation in Supplementary Fig. S5.

It is important to note that the *J*–*V* curves presented in this work were measured after aging the samples under constant light

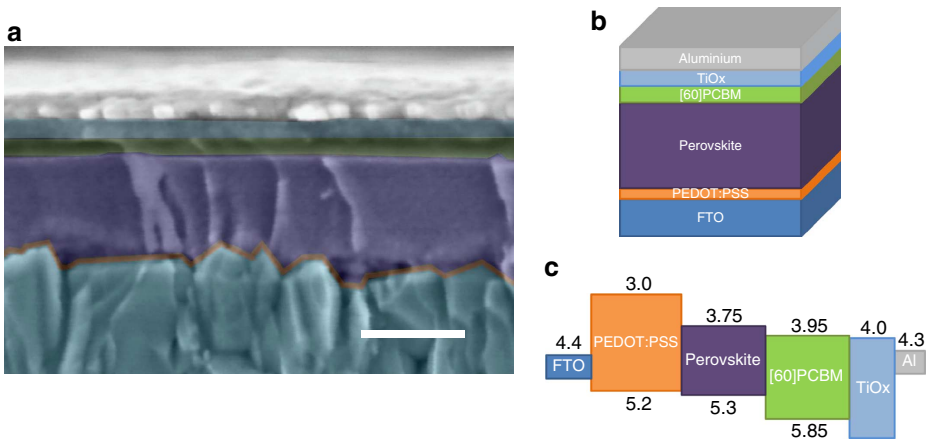

Figure 2 | Optimized device structure. (**a**) SEM. cross-sectional image of the optimized inverted device configuration. Scale bar represents 250 nm. The different layers have been tinted with the colour scheme of the device schematic shown in (**b**). (**c**) Approximate energy band diagram of the fabricated inverted structure taken from reference[21].

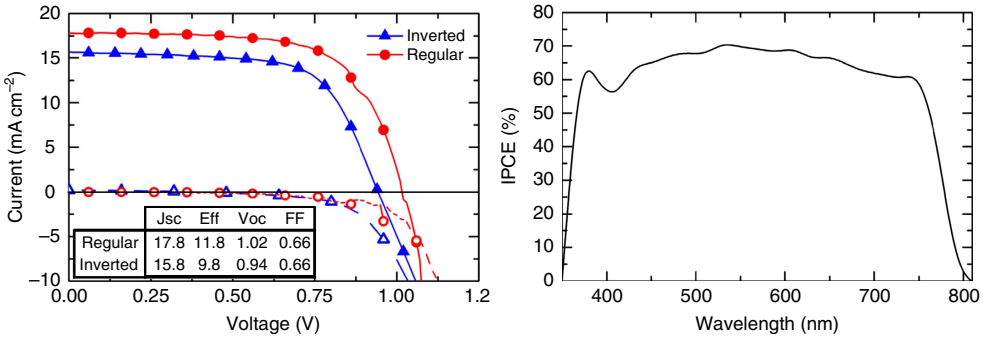

Figure 3 | Photovoltaic performance characteristics. (**a**) Current voltage curves for champion devices of regular MSSC (red circles) and inverted planar-heterojunction (blue triangles) configuration. Inset shows the short-circuit current density (J_{sc}, mA cm^{-2}), power-conversion efficiency (Eff, %), open-circuit voltage (V_{oc}, V) and FF for both device architectures. (**b**) Incident photon-to-electron conversion efficiency against wavelength for a typical inverted device. The integrated current from the product of the incident photon-to-electron conversion efficiency and the AM 1.5 100 mW cm^{-2} solar spectrum is 16.5 mA cm^{-2}, in close agreement to the short-circuit photocurrent measured under simulated sunlight.

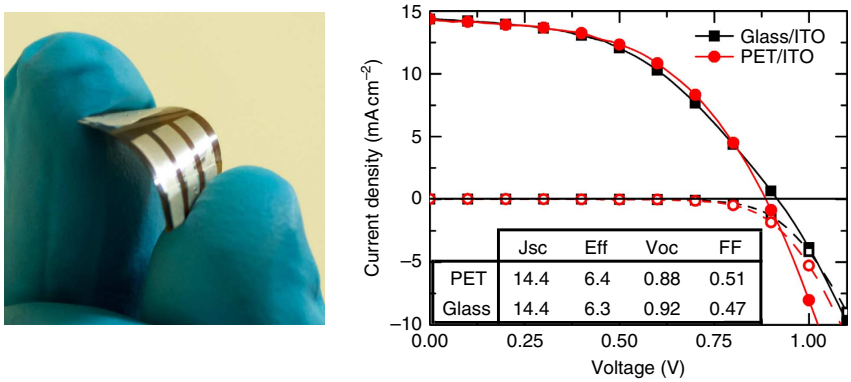

Figure 4 | Flexible solar cell performance. (**a**) Picture of the first flexible perovskite solar cell and (**b**) *J*–*V* curves for inverted architecture devices fabricated both on ITO-covered glass and PET, measured under-simulated AM 1.5 100 mW cm^{-2} sunlight. The inset table shows the photovoltaic performance parameters, J_{sc} (mA cm^{-2}), efficiency (%), V_{oc} (V) and FF.

illumination for a number of minutes. The initial current voltage curve typically exhibit a little over >1% PCE, but increased to between 7.5–10% after around 10 minutes of constant illumination and operation in air (Supplementary Fig. S6). This is not the case for the regular MSSC that operates well immediately. The requirement for light soaking of TiO_x is consistent with previous reports in organic photovoltaics[26].

Flexible solar cells. Finally, enabled by the 'all low-temperature' processing, we have also fabricated inverted perovskite devices on ITO-coated poly(ethylene terephthalate) (PET) substrates, shown in Fig. 4. Devices fabricated on either ITO-covered glass or PET exhibited essentially the same photovoltaic performance parameters, with short-circuit currents of over 14 mA cm^{-2}, open-circuit voltages of around 0.9 V and power-conversion efficiencies of over 6.3%. The main difference between devices fabricated on ITO- and FTO-covered glass is the lower fill factor (FF) and current of the ITO devices. This may in part be accommodated by the batch–to-batch variation, but is likely to also arise from poorer perovskite film formation and lower surface coverage upon the PEDOT:PSS-coated ITO as opposed to the PEDOT:PSS-coated FTO, as shown in Supplementary Fig. S7. The main difference between FTO and ITO is the surface roughness, with the latter being much smoother. It is likely that the roughness of the FTO is an important factor in enabling more uniform perovskite coating and ensuing better operation of these inverted perovskite solar cells, which do not incorporate any mesoporous scaffold.